From Intramolecularly [4 + 1]- and [4 + 2]-Coordinated Tri- and Tetraorganosilanes to Hypercoordinated Benzoxasilaphospholes†

Katja Peveling,‡ Markus Schürmann,‡ Ralf Ludwig,§ and Klaus Jurkschat*,‡

Lehrstuhl für Anorganische Chemie II der Universität Dortmund and Physikalische Chemie der Universität Dortmund, D-44221 Dortmund, Germany

Received April 23, 2001

The synthesis of the intramolecularly coordinated triorganosilane {4-*t*-Bu-2,6-[P(O)(OEt)$_2$]$_2$C$_6$H$_2$}Si(H)Ph$_2$ (**3**) is reported. The reaction of both **3** and the corresponding tetraorganosilane {4-*t*-Bu-2,6-[P(O)(OEt)$_2$]$_2$C$_6$H$_2$}SiPh$_3$ (**2**) with [Ph$_3$C]$^+$[PF$_6$]$^-$ results in the in situ generation of the siliconium ion {4-*t*-Bu-2,6-[P(O)(OEt)$_2$]$_2$C$_6$H$_2$}SiPh$_2^+$PF$_6^-$ (**4**). The siliconium ion of **4** reacts with water under intramolecular cyclization to give the novel hypercoordinated benzoxasilaphosphole [1(*P*),3(*Si*)-P(O)(OEt)OSiPh$_2$-6-*t*-Bu-4-P(O)(OEt)$_2$]-C$_6$H$_2$ (**5**). Compound **5** and the related methyl/phenyl- and dimethyl-substituted derivatives [1(*P*),3(*Si*)-P(O)(OEt)OSiRR′-6-*t*-Bu-4-P(O)(OEt)$_2$]C$_6$H$_2$ (**6**, R = Me, R′ = Ph; **7**, R = R′ = Me) are also prepared by reaction of {4-*t*-Bu-2,6-[P(O)(OEt)$_2$]$_2$C$_6$H$_2$}Li (**1**) with the corresponding dichlorodiorganosilanes. Compound **6** is a mixture of diastereomers from which the 1*S**,3*S** diastereomer **6a** was separated. In solution, the latter undergoes an acid-catalyzed epimerization which was monitored by ^{31}P NMR spectroscopy. The mechanism proposed to account for this process is supported by ab initio MO calculations. The molecular structures of **3**, **5**, and **6a** were determined by single-crystal X-ray diffraction.

Introduction

Hypercoordinated inorganic silicon as well as organosilicon compounds have been and still are very attractive subjects for a great number of chemists, and this is mainly because of structural aspects and unexpected reactivity patterns associated with these compounds.[1,2]

Interestingly, mainly nitrogen-containing ligands have been employed for the synthesis of intramolecularly coordinated organosilicon compounds, and the most prominent representatives of these are the so-called silatranes and their analogues[3,4] and compounds containing built-in ligands of types **A**[5−14] and **E**[15−21] (Chart 1). On the other hand, fewer examples for intramolecularly coordinated silicon compounds involving phosphorus- (**B**,[22−26] **F**[24]), oxygen- (**C**[25−27]), and sulfur-containing ligands (**D**[25,26]) are known (Chart 1).

Recently, we reported the O,C,O-coordinating pincer-type ligand **G** and its application to the synthesis of intramolecularly coordinated organotin compounds.[28−30] An interesting aspect in the chemistry of ligand **G** is that, in addition to its strong donor capacity, a variety of reactions are possible not only at the metal atom it

† Parts of these results were first presented at the 13th FECHEM Conference on Organometallic Chemistry, Aug 29−Sept 3, 1999, Lisbon, Portugal, Book of Abstracts p 54, and at the 33rd ACS Organosilicon Symposium, April 7−8, 2000, Saginaw Valley State University, Saginaw, MI, Book of Abstracts PA 29.

‡ Lehrstuhl für Anorganische Chemie II der Universität Dortmund.

§ Physikalische Chemie der Universität Dortmund.

(1) (a) Chuit, C.; Corriu, R. J. P.; Reyé, C. Structure and Reactivity of Hypercoordinate Silicon Species. In *Chemistry of Hypervalent Compounds*; Akiba, K.-y., Ed.; Wiley-VCH: Weinheim, Germany, 1999, and references cited therein. (b) Kira, M.; Zhang, L. C. Hypercoordinate Silicon Species in Organic Synthesis. In *Chemistry of Hypervalent Compounds*; Akiba, K.-y., Ed.; Wiley-VCH: Weinheim, Germany, 1999, and references cited therein.

(2) Brook, M. A. *Silicon in Organic, Organometallic, and Polymer Chemistry*; Wiley: New York, 2000.

(3) Yoshikawa, A.; Gordon, M. S.; Sidorkin, V. F.; Pestunovich, V. A. *Organometallics* **2001**, *20*, 927.

(4) Timosheva, N. V.; Chandrasekaran, A.; Day, R. O.; Holmes, R. R. *Organometallics* **2000**, *19*, 5614 and references cited therein.

(5) Weinmann, M.; Gehrig, A.; Schiemenz, B.; Huttner, G.; Nuber, B.; Rheinwald, G.; Lang, H. *J. Organomet. Chem.* **1998**, *563*, 61.

(6) Auner, N.; Probst, R.; Hahn, F.; Herdtweck, E. *J. Organomet. Chem.* **1993**, *459*, 25.

(7) Timosheva, N. V.; Chandrasekaran, A.; Day, R. O.; Holmes, R. R. *Organometallics* **2001**, *20*, 2331.

(8) Chandrasekaran, A.; Day, R. O.; Holmes, R. R. *J. Am. Chem. Soc.* **2000**, *122*, 1066.

(9) Chuit, C.; Corriu, R. J. P.; Reyé, C.; Young, J. C. *Chem. Rev.* **1993**, *93*, 1371.

(10) Belzner, J.; Ronneberger, V.; Schär, D.; Brönnecke, C.; Herbst-Irmer, R.; Noltemeyer, M. *J. Organomet. Chem.* **1999**, *577*, 330.

(11) Corriu, R. J. P.; Lanneau, G. F.; Perrot-Petta, M.; Mehta, V. D. *Tetrahedron Lett.* **1990**, *31*, 2585.

(12) Corriu, R. J. P.; Kpoton, A.; Poirier, M.; Royo, G.; De Saxcé, A.; Young, J. C. *J. Organomet. Chem.* **1990**, *395*, 1.

(13) Belzner, J.; Schär, D.; Kneisel, B. O.; Herbst-Irmer, R. *Organometallics* **1995**, *14*, 1840.

(14) Brelière, C.; Carré, F.; Corriu, R. J. P.; Royo, G.; Man, M. W. C.; Lapasset, J. *Organometallics* **1994**, *13*, 307.

(15) Chauhan, M.; Chuit, C.; Corriu, R. J. P.; Reyé, C. *Tetrahedron Lett.* **1996**, *37*, 845.

(16) Chauhan, M.; Chuit, C.; Corriu, R. J. P.; Mehdi, A.; Reyé, C. *Organometallics* **1996**, *15*, 4326.

(17) Carré, F.; Chuit, C.; Corriu, R. J. P.; Mehdi, A.; Reyé, C. *Angew. Chem.* **1994**, *106*, 1152.

(18) Carré, F.; Chauhan, M.; Chuit, C.; Corriu, R. J. P.; Reyé, C. *J. Organomet. Chem.* **1997**, *540*, 175.

(19) Chuit, C.; Corriu, R. J. P.; Mehdi, A.; Reyé, C. *Angew. Chem.* **1993**, *105*, 1372.

(20) Carré, F.; Chuit, C.; Corriu, R. J. P.; Mehdi, A.; Reyé, C. *Organometallics* **1995**, *14*, 2754.

(21) Carré, F.; Chuit, C.; Corriu, R. J. P.; Fanta, A.; Mehdi, A.; Reyé, C. *Organometallics* **1995**, *14*, 194.

10.1021/om010334c CCC: $20.00
Publication on Web 09/20/2001

Chart 1

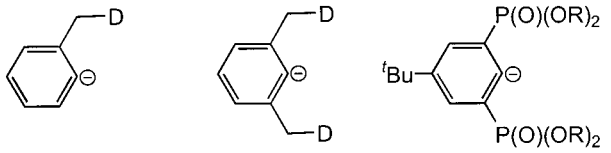

A, D = NMe_2
B, D = PR_2
C, D = OR
D, D = SR

E, D = NMe_2
F, D = PR_2

G (R = Et, *i*-Pr)

is attached to but also at the phosphonyl moieties. For instance, the attempt to prepare the intramolecularly hexacoordinated triorganotin halide {4-*t*-Bu-2,6-[P(O)-$(OEt)_2]_2C_6H_2$}$SnXPh_2$ (X = Cl, Br, I) by reaction of the corresponding triphenyltin derivative with hydrogen chloride or bromine and iodine, respectively, gave the novel intramolecularly coordinated benzoxaphosphastannole [1(*Sn*),3(*P*)-$Ph_2SnOP(O)(OEt)$-5-*t*-Bu-7-P(O)-$(OEt)_2]C_6H_2$ instead.[29]

In preliminary communications, we also reported the synthesis and structure of the first [4 + 2]-coordinated tetraorganosilicon compounds containing these ligands, namely {4-*t*-Bu-2,6-$[P(O)(OR)_2]_2C_6H_2$}$SiPh_3$ (R = Et, *i*-Pr).[31,32]

In continuation of this work we present here the synthesis, structure, and reactivity of the hypercoordinated tetra- and triorganosilicon compounds **2** and **3**, show their transformation into the intramolecularly coordinated benzoxasilaphosphole **5**, and, in addition, synthesize the related methyl/phenyl- and dimethyl-substituted derivatives **6** and **7**, respectively. Furthermore, we have studied the epimerization of the 1*S**,3*S** diastereomer **6a** and propose an acid-catalyzed mechanism to account for this process. The experimental investigations are accompanied by ab initio MO calculations.

Results and Discussion

The tetraorganosilane **2**[32] and the triorganosilane **3** were obtained as colorless crystals in poor to good yields by reaction of the in situ generated organolithium compound **1** with the chloroorganosilanes Ph_3SiCl and $Ph_2Si(H)Cl$, respectively (eq 1).

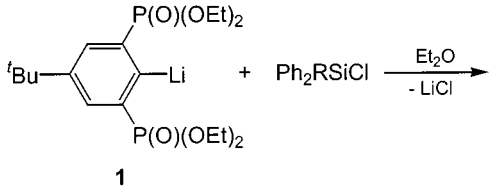

1

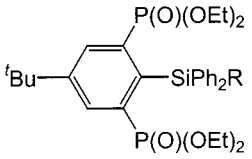

2, R = Ph[32]
3, R = H

(1)

The molecular structure of compound **3** is shown in Figure 1, selected geometrical data are given in Table 1, and relevant crystallographic parameters are listed in Table 3.

In contrast to its triphenyl-substituted analogue **2**,[32] in the triorganosilane **3** one P=O group points away from the silicon atom, with the consequence that the latter adopts a distorted-trigonal-bipyramidal configuration (geometrical goodness[33−35] $\Delta\Sigma(\theta) = 30.9°$) with C(1), C(11), and C(21) in equatorial and O(2) and H(1) in axial positions. The intramolecular Si(1)−O(2) distance amounts to 2.918(2) Å and reflects a Pauling-type bond order[36−38] (BO) of 0.02. It is shorter than the Si−O distances of 3.122(3) and 3.158(2) Å in the [4 + 2]-coordinated tetraorganosilane **2**.[32]

The Si(1)−H(1) distance of 1.42(2) Å is in the range of Si−H distances in hypercoordinated silanes containing nitrogen donors such as $C_6H_4\{SiH_2[C_6H_3(CH_2NMe_2)_2\text{-}2,6]_2\text{-}1,4\}_2$ (Si−H = 1.42(2), 1.44(2) Å)[20] and $[C_6H_3(CH_2NMe_2)_2\text{-}2,6]_2SiH_2$ (Si−H = 1.44(4) Å).[17] In addition, there are intramolecular H(1)···O(1′) and H(1)···O(1″) distances of 2.47(2) and 2.51(2) Å, respectively. Although these distances are shorter than the sum of the van der Waals radii of hydrogen (1.4 Å) and oxygen (1.5 Å)[39] and hence suggest hydrogen bonding, neither these distances nor the weak intramolecular Si···O coordination seems to influence the Si(1)−H(1) bond length.

In contrast, when we consider the relation between $\tilde{\nu}$ and the force constant,[40] the IR spectrum ($\tilde{\nu}$(Si−H) 2198 cm^{-1}) indicates the Si−H bond in **3** to be even deactivated in comparison with the corresponding bond in tetracoordinated triphenylsilane, Ph_3SiH ($\tilde{\nu}$(Si−H) 2121 cm^{-1}).

The $^1J(^{29}Si-^1H)$ value of 196 Hz in the triorganosilane **3** (Table 2) is almost identical with the $^1J(^{29}Si-^1H)$ value of 198 Hz in the tetracoordinated triphenylsilane, Ph_3-

(22) Gossage, R. A.; McLennan, G. D.; Stobart, S. R. *Inorg. Chem.* **1996**, *35*, 1729.
(23) Abicht, H. P.; Issleib, K. *Z. Anorg. Allg. Chem.* **1976**, *422*.
(24) Müller, G.; Waldkircher, M.; Pape, A. Phosphine Coordination to Silicon Revisited. In *Organosilicon Chemistry III*; Auner, N., Weiss, J., Eds.; Wiley-VCH: Weinheim, Germany, 1998; p 452.
(25) Berlekamp, U. H.; Mix, A.; Jutzi, P.; Stammler, H. G.; Neumann, B. Oxygen, Phosphorus or Sulfur Donor Ligands in Higher-coordinated Organosilyl Chlorides and Triflates. In *Organosilicon Chemistry IV*; Auner, N.;, Weiss, J., Eds.; Wiley-VCH: Weinheim, Germany, 2000; p 489.
(26) Berlekamp, U.-H.; Jutzi, P.; Mix, A.; Neumann, B.; Stammler, H.-G.; Schoeller, W. W. *Angew. Chem.* **1999**, *111*, 2071.
(27) Mix, A.; Berlekamp, U. H.; Stammler, H.-G.; Neumann, B.; Jutzi, P. *J. Organomet. Chem.* **1996**, *521*, 177.
(28) Mehring, M.; Schürmann, M.; Jurkschat, K. *Organometallics* **1998**, *17*, 1227.
(29) Mehring, M.; Löw, C.; Schürmann, M.; Jurkschat, K. *Eur. J. Inorg. Chem.* **1999**, 887.
(30) Mehring, M.; Löw, C.; Schürmann, M.; Uhlig, F.; Jurkschat, K.; Mahieu, B. *Organometallics* **2000**, *19*, 4613.
(31) Peveling, K.; Schürmann, M.; Jurkschat, K. *Main Group Met. Chem.* **2001**, *24*, 251.
(32) Mehring, M.; Jurkschat, K.; Schürmann, M. *Main Group Met. Chem.* **1998**, *21*, 635.
(33) Kolb, U.; Dräger, M.; Jousseaume, B. *Organometallics* **1991**, *10*, 2737.
(34) Kolb, U.; Beuter, M.; Dräger, M. *Inorg. Chem.* **1994**, *33*, 4522.
(35) Kolb, U.; Beuter, M.; Gerner, M.; Dräger, M. *Organometallics* **1994**, *13*, 4413.
(36) Pauling, L. *The Nature of the Chemical Bond*, 3rd ed.; Cornell University Press: Ithaca, NY, 1960.
(37) Dunitz, J. D. *X-ray Analysis and the Structure of Organic Molecules*; Cornell University Press: Ithaca, NY, 1979.
(38) Huheey, J.; Keiter, E. A.; Keiter, R. L. *Anorganische Chemie: Prinzipien von Struktur und Reaktivität*, 2nd ed.; de Gruyter, New York, Berlin, 1995.
(39) Hollemann, A. F.; Wiberg, N. *Lehrbuch der Anorganischen Chemie*, 101st ed.; de Gruyter: Berlin, New York, 1995.
(40) Schrader, B. *Infrared and Raman Spectroscopy: Methods and Applications*; VCH: Weinheim, New York, 1995.

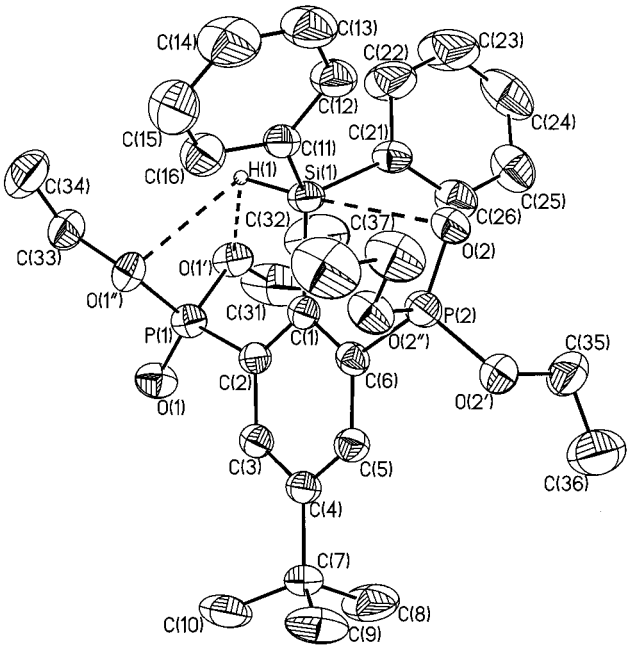

Figure 1. General view (SHELXTL) of a molecule of **3** showing 30% probability displacement ellipsoids and the atom numbering.

SiH, indicating no or little difference in the s character[41] of these Si−H bonds.

On the other hand, however, the low-frequency ^{29}Si chemical shift of δ −25.6 for **3** in comparison to δ −17.7 for Ph_3SiH[42] and δ −25.7 for $[C_{10}H_5(NMe_2)_2$-4,8]$SiPh_2H$[43] reflects the [4 + 1] coordination in compound **3**.[44,45]

The ^{31}P NMR spectrum at room temperature of **3** shows a single resonance at δ 19.8 which is shifted to slightly higher frequency than the signal of the phosphonate precursor {5-*t*-Bu-1,3-$[P(O)(OEt)_2]_2C_6H_3$} (δ 18.9)[28] and of compound **2** (δ 19.1),[32] respectively, indicating both phosphorus atoms to be equivalent on the ^{31}P NMR time scale.

At −75 °C, however, decoalescence of the signal into two resonances of equal integral (δ 19.4, 19.2) takes place with the rotation about the P−C bond becoming slow.

To get an idea whether the solid-state structures of the tetraorganosilane **2** and of the triorganosilane **3** are influenced by crystal-packing effects and why in compound **3** one of the two P═O groups points away from the silicon atom, ab initio MO calculations have been performed. The geometry-optimized structure for compound **2** is almost identical with the structure actually observed in the solid state, especially in the essential point that both P═O groups point toward the silicon atom (see the Supporting Information). For compound **3**, the solid-state structure and the geometry-optimized structure with input data based on the former also show a rather good agreement (Table 1). To estimate whether the solid-state structure as determined by single-crystal X-ray analysis is indeed the thermodynamically most stable one, the hypothetical structure **3′** was created by rotating the P(1)-containing phosphonyl group about the P(1)−C(2) bond to the extent that the P═O group points to the silicon center (Figure 2, left).

Geometry optimization of this structure revealed a partial reorientation of this phosphonyl group to a geometry where the P═O group again points away from the silicon atom. This reorientation is associated with

Table 1. Selected Bond Lengths (Å), Bond Angles (deg), and Torsion Angles (deg) for 3, for the Geometry-Optimized Structure of 3 (RHF 6-31G*), for the Hypothetical [4+2]-Coordinated Structure 3′, and for the Geometry-Optimized Structure of 3′ (RHF 3-21 G)

	3	**3** (RHF 6-21G*)	**3′**	**3′** (RHF 3-21 G)
Si(1)−C(1)	1.913(3)	1.944	1.970	1.972
Si(1)−C(11)	1.861(3)	1.893	1.908	1.905
Si(1)−C(21)	1.859(3)	1.887	1.909	1.903
Si(1)−O(2)	2.918(2)	3.031	3.087	2.739
Si(1)−O(1)			3.019	3.605
Si(1)−O(1″)			4.623	3.628
Si(1)−H(1)	1.42(2)	1.46	1.466	1.472
P(1)−O(1)	1.467(2)	1.461	1.543	1.547
P(2)−O(2)	1.460(2)	1.459	1.545	1.547
P(1)−O(1′)	1.577(2)	1.585	1.637	1.639
P(1)−O(1″)	1.560(2)	1.578	1.625	1.635
P(2)−O(2′)	1.569(2)	1.592	1.635	1.631
P(2)−O(2″)	1.572(2)	1.573	1.622	1.622
O(1′)−H(1)	2.47(2)	2.61	4.130	4.247
O(1″)−H(1)	2.51(2)	2.54	3.780	2.555
C(11)−Si(1)−C(1)	113.4(2)	113.3	111.2	109.9
C(21)−Si(1)−C(1)	114.9(2)	114.9	117.2	116.1
C(21)−Si(1)−C(11)	114.7(1)	114.7	117.1	124.2
O(1)−P(1)−C(2)	112.6(1)	112.2	112.0	121.5
C(1)−Si(1)−O(2)	78.86(9)	76.1	78.0	81.1
C(11)−Si(1)−O(2)	73.9(1)	74.7	72.5	76.4
C(21)−Si(1)−O(2)	75.1(1)	76.9	80.7	81.0
C(1)−Si(1)−O(1)			79.7	74.6
H(1)−Si(1)−C(1)	105.4(8)	104.4	103.3	99.5
H(1)−Si(1)−C(11)	103.6(8)	102.0	111.2	109.9
H(1)−Si(1)−C(21)	103.1(8)	105.8	103.3	116.1
P(2)−O(2)−Si(1)	95.80(9)	94.3	90.9	100.4
H(1)−Si(1)−O(2)	175.8(8)	176.5	174.4	177.0
H(1)−Si(1)−O(1)			35.1	38.1
C(6)−C(1)−Si(1)	123.0(2)	123.3	124.0	123.3
C(1)−C(6)−P(2)	121.3(2)	122.6	122.6	120.0
C(6)−P(2)−O(2)	113.0(1)	113.5	115.9	112.7
C(1)−C(2)−P(1)	126.6(2)	127.3	127.8	124.2
C(2)−C(1)−Si(1)	122.2(2)	121.3	120.8	121.1
Si(1)−H(1)-O(1′)	114(9)	102.6	102.6	113.7
Si(1)−H(1)-O(1″)	120(1)	126.0	116.5	126.5
O(1′)-H(1)−O(1″)	59.4(5)	57.5	39.6	34.6
P(1)−C(2)−C(1)−Si(1)	−3.2(3)	8.4	0.9	1.1
P(2)−C(6)−C(1)−Si(1)	1.6(3)	−10.1	−0.8	−0.2
C(5)−C(6)−P(2)−O(2)	153.1(2)	155.0	115.7	166.2
C(3)−C(2)−C(1)−Si(1)	178.0(2)	−173.7	−179.7	−179.6
C(3)−C(2)−P(1)−O(1)	−5.2(2)	−13.9	−162.5	−122.3
C(2)−C(1)−Si(1)−H(1)	11.7(8)	17.6	18.2	9.8

Table 2. Selected ^{29}Si and ^{31}P NMR Data for G-H (R = Et), 2, 3, 4, 5, 6a, and 7

	$\delta(^{31}P)$	$\delta(^{29}Si)$	$J(^{31}P-^{29}Si)$	$^4J(^{31}P-^{31}P)$	$^1J(^{29}Si-^1H)$
G-H[28,a]	18.9				
2[32,a]	19.1	−16.3	6		
3	19.8[a]	−25.3[b]	5[b]		196[b]
4[c]	29.6	−67.9	2		
5[a]	21.5/22.4	−24.7	3/7	6	
6a[a]	21.7/22.1	−5.3	3/6	6	
7	19.9/21.8[c]	10.5[a]	3/6[a]	6[c]	

[a] In $CDCl_3$, [b] In CH_2Cl_2/D_2O-capillary. [c] In C_6D_6.

(41) Harris, R. K.; Mann, B. E. *NMR and the Periodic Table*; Academic Press: London, 1978.
(42) Olah, G. A.; Hunadi, R. J. *J. Am. Chem. Soc.* **1980**, *102*, 6989.
(43) Brelière, C.; Corriu, R. J. P.; Royo, G.; Man, M. W. C.; Zwecker, J. *C.R. Acad. Sci. Paris* **1991**, *313*, 1527.
(44) Marsmann, H. C. Silicon-29 NMR. In *Encyclopedia of Nuclear Magnetic Resonance*; Grant, D. M., Harris, R. K., Eds.; Wiley: Chichester, U.K., 1996; Vol. 7, p 4386.
(45) Bassindale, A. R.; Jiang, J. *J. Organomet. Chem.* **1993**, *446*, C3.

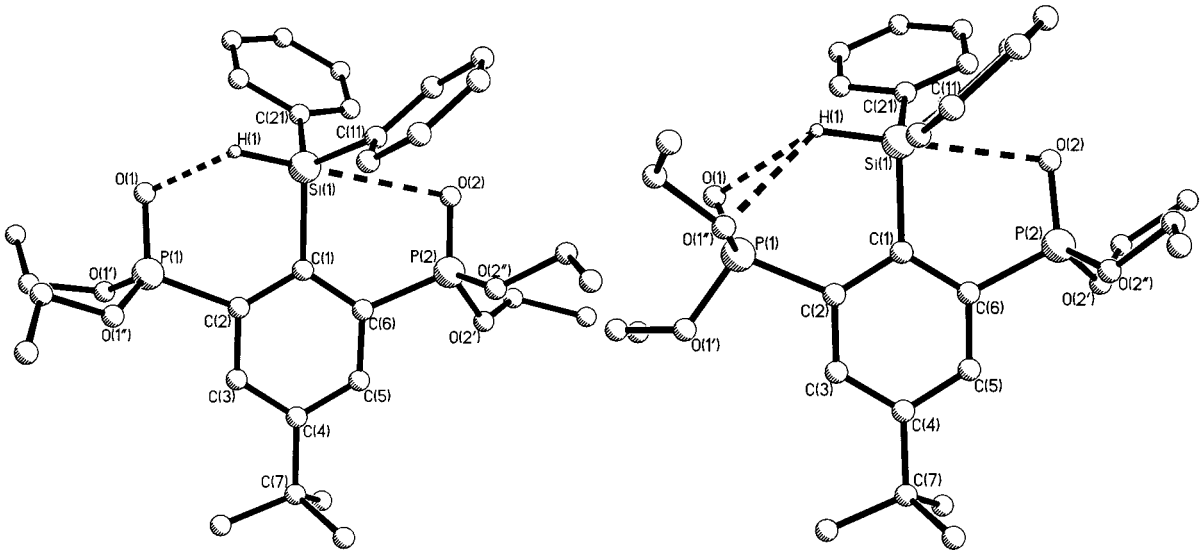

Figure 2. General view (SHELXTL) of a hypothetical molecule of **3′** (left hand) and of its geometry-optimized structure (right hand).

Scheme 1

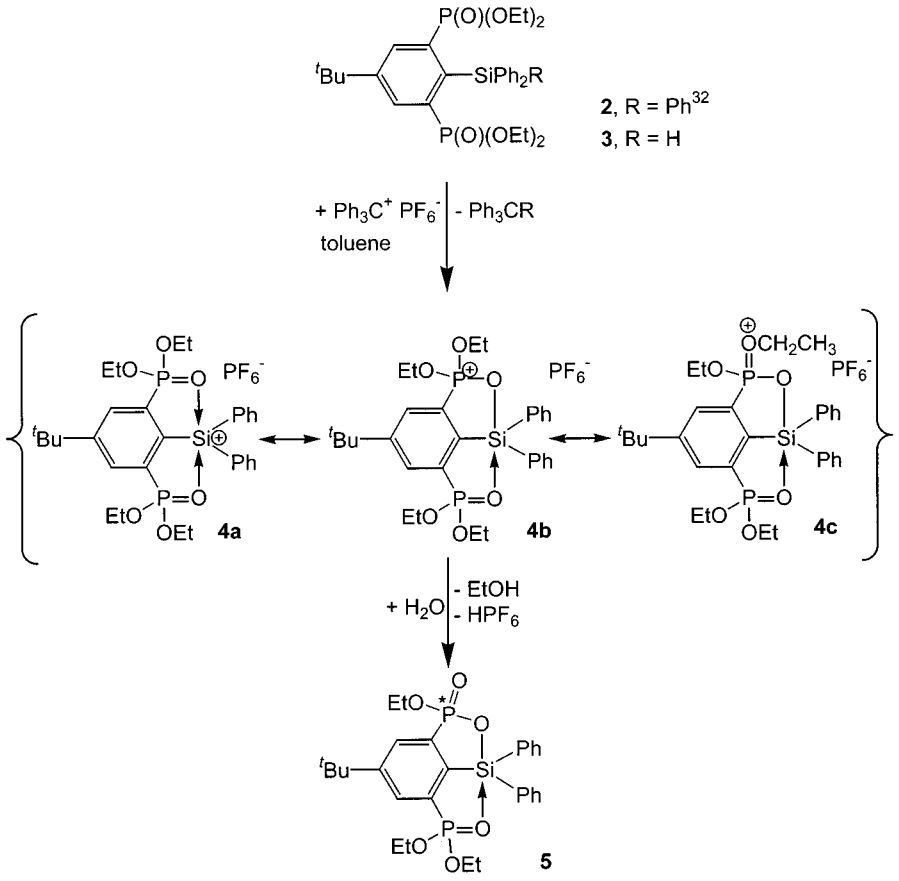

an energy gain of 18.4 kJ/mol. However, in this optimized structure of **3′** the reorientation is not complete, as further rotation to reach the structure actually observed in the solid state is prevented by steric hindrance between the phosphonyl and the phenyl groups (Figure 2, right). This is in line with the hindered rotation about the P−C bond as observed in the low-temperature ^{31}P NMR spectra (see above).

The attempt at converting the Si−H function in the silane **3** into an Si−Cl function by reaction of **3** with CCl_4 failed.

The organosilicon derivatives **2** and **3** were converted in situ into the corresponding pentacoordinated organosiliconium ion **4** by reaction with $Ph_3C^+PF_6^-$ (Scheme 1).

The identity of compound **4** follows from the low-frequency triplet resonance at δ −67.9 ($J(^{29}Si-^{31}P) = 2$ Hz) in the ^{29}Si NMR spectrum (Table 2). Comparable compounds are $[C_6H_3(CH_2NMe_2)_2\text{-}2,6]SiHPh^+$ (δ −29.7),[19] $[C_6H_3(CH_2NMe_2)_2\text{-}2,6]SiMePh^+$ (δ −15.0),[15,16] $[C_6H_3(CH_2NMe_2)_2\text{-}2,6]SiMe_2^+$ (δ −25.0),[19] and $[C_6H_4(CH_2OMe)\text{-}2]_2SiH^+$ (δ −47.2).[26] The high-frequency ^{31}P chemical

Table 3. Crystallographic Data for 3, 5, and 6a

	3	5	6a
formula	$C_{30}H_{42}O_6P_2Si$	$C_{28}H_{36}O_6P_2Si{\cdot}0.5H_2O$	$C_{23}H_{34}O_6P_2Si$
fw	588.67	567.61	496.53
cryst syst	monoclinic	monoclinic	monoclinic
cryst size, mm	0.25 × 0.20 × 0.20	0.1 × 0.08 × 0.08	0.20 × 0.05 × 0.05
space group	$P2_1/n$	$P2_1/n$	$C2/c$
a, Å	10.037(1)	12.230(1)	18.536(1)
b, Å	24.696(1)	14.544(1)	18.717(1)
c, Å	13.874(1)	17.126(1)	17.377(1)
α, deg	90	90	90
β, deg	105.336(1)	94.776(1)	117.810(1)
γ, deg	90	90	90
V, Å^3	3316.5(4)	3035.7(4)	5332.4(5)
Z	4	4	8
ρ_{calcd}, Mg/m^3	1.179	1.242	1.237
μ, mm^{-1}	0.205	0.222	0.242
F(000)	1256	1204	2112
θ range, deg	3.02−27.47	3.43−25.01	3.43−25.34
index ranges	$-13 \le h \le 13$	$-14 \le h \le 14$	$-22 \le h \le 22$
	$-32 \le k \le 32$	$-14 \le k \le 14$	$-22 \le k \le 22$
	$-18 \le l \le 17$	$-20 \le l \le 20$	$-17 \le l \le 17$
no. of rflns collcd	42 617	38 042	35 302
completeness to θ_{max}	99.8	93.1	93.5
no. of indep rflns/R_{int}	7572/0.046	4983/0.033	4566/0.029
no. of rflns obsd ($I > 2\sigma(I)$)	2821	2037	2699
no. of refined params	385	362	325
GOF(F^2)	0.809	0.835	0.900
R1(F) ($I > 2\sigma(I)$)	0.0494	0.0549	0.0432
wR2(F^2) (all data)	0.1348	0.1601	0.1212
$(\Delta/\sigma)_{max}$	0.001	< 0.001	< 0.001
largest diff peak/hole, e/Å^3	0.471/−0.218	0.290/−0.207	0.306/−0.234

Scheme 2

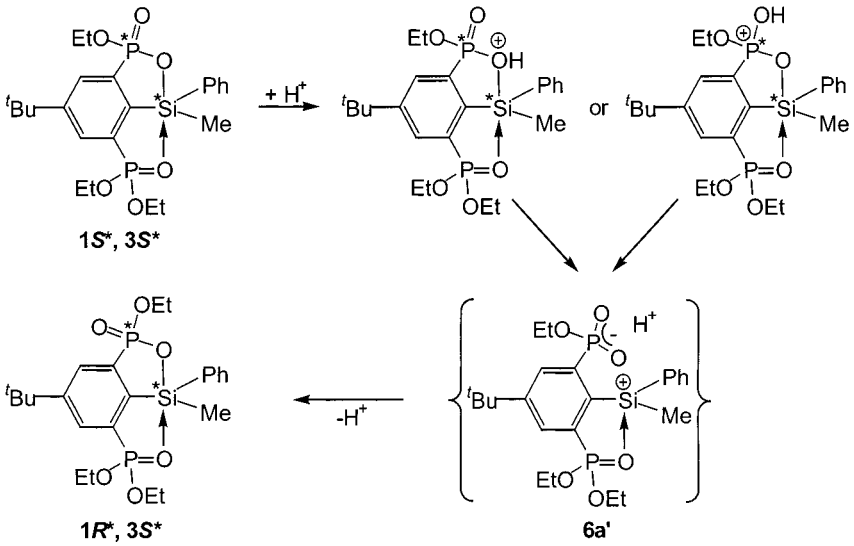

shift for compound **4** (δ 29.6) is comparable with that of the corresponding organotin cation {4-*t*-Bu-2,6-[P(O)-(O^{i}Pr)$_2$]$_2$C$_6$H$_2$}SnPh$_2^+$PF$_6^-$ (δ 26.1).[46]

Upon contact with air moisture or by addition of water to the reaction mixture, the organosilicon cation **4** was converted into the intramolecularly coordinated benzoxasilaphosphole derivative **5** (Scheme 1).

The formation of the benzoxasilaphosphole **5** can formally be rationalized by nucleophilic attack of a water molecule either at the positively charged phosphorus atom in the mesomeric formula **4b** or at the methylene carbon of the ethoxy group in the mesomeric formula **4c**, followed by release of ethanol and deprotonation (Scheme 1). The driving force for the cyclization is the formation of the O−Si bond.

In addition to the signal attributed to compound **5**, the ^{29}Si NMR spectrum of the crude reaction mixture showed single resonances at δ −19.8, −21.2, −21.5, and −21.6 which were not assigned.

A detailed mechanistic study on the formation of compound **5** and related organotin derivatives[29] will be a subject of a forthcoming paper.

An alternative synthesis for compound **5** and its related derivatives **6** and **7** is the one-pot reaction of the organolithium compound **1** with the corresponding dichlorodiorganosilanes (eq 2).

Compound **5** is a colorless solid, whereas compounds **6** (mixture of two diastereomers) and **7** are colorless oils. After recrystallization of compound **6** from hexane the

(46) Löw, C.; Mehring, M.; Jurkschat, K.; Schürmann, M. To be submitted for publication.

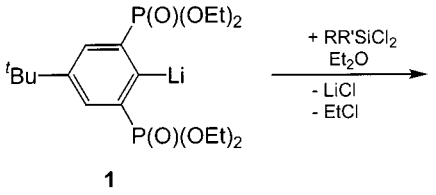

1

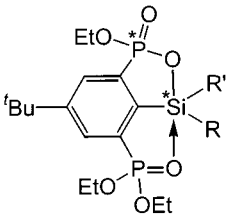

(2)

5, R = R' = Ph
6, R = Ph, R' = Me
7, R = R' = Me

1*S**,3*S** diastereomer, hereafter referred to as **6a**, was obtained as a colorless solid (see below).

Mechanistically, the formation of the benzoxasilaphospholes **5**−**7** according to eq 2 can be rationalized in analogy to the corresponding organotin derivatives:[29] i.e., via the intermediate generation of hypercoordinated siliconium ions followed by nucleophilic attack of chloride ion at the methylene carbon of the ethoxy group (mesomeric formula **4c** in Scheme 1) and release of ethyl chloride.

Benzoxasilaphospholes containing tetracoordinated silicon have been prepared by reaction of the corresponding phosphasiletene with oxygen.[47,48]

The molecular structures of compounds **5** and **6a** are shown in Figures 3 and 4, respectively, and selected geometrical data are given in Table 4.

In both benzoxasilaphospholes **5** and **6a** the silicon atoms adopt a distorted-trigonal-bipyramidal configuration (geometrical goodness[33−35] $\Delta\Sigma(\theta)$ = 53.9 and 55.0°, respectively), with O(1) and O(2′) occupying the axial positions and C(1), C(11), and C(21) occupying the equatorial positions. The O(1)−Si(1)−O(2') angles amount to 168.2(1)° (**5**) and 169.32(8)° (**6a**), respectively, which is about 10° larger than the corresponding angle in the related benzoxaphosphastannole.[29] The displacement of the silicon atoms from the trigonal planes defined by C(1), C(11), and C(21) amounts to 0.298(3) Å (**5**) and 0.305(2) Å (**6a**) in the direction of O(2'). The Si(1)−O(1) distances of 2.672(3) Å (**5**) and 2.614(2) Å (**6a**), respectively, are significantly shorter than the intramolecular Si−O distances in the tetraorganosilicon compound **2** (3.158(2), 3.122(3) Å).[32] The Si(1)−O(2') bond lengths amount to 1.715(3) Å (**5**) and 1.718(2) Å (**6a**), respectively.

Consequently, the hypercoordinated benzoxasilaphospholes **5** and **6a** can be seen as representatives of the type I mesomeric formula, whereas their related organotin[29] and organolead[49] derivatives are close to the mesomeric formula II (Chart 2). Ab initio MO calculations based on the coordinates as obtained by single-crystal X-ray analysis gave a geometry-optimized structure for **6a** in which the coordinative Si(1)−O(1) bond is elongated by 0.26 Å as compared to the solid-state structure (Table 4).

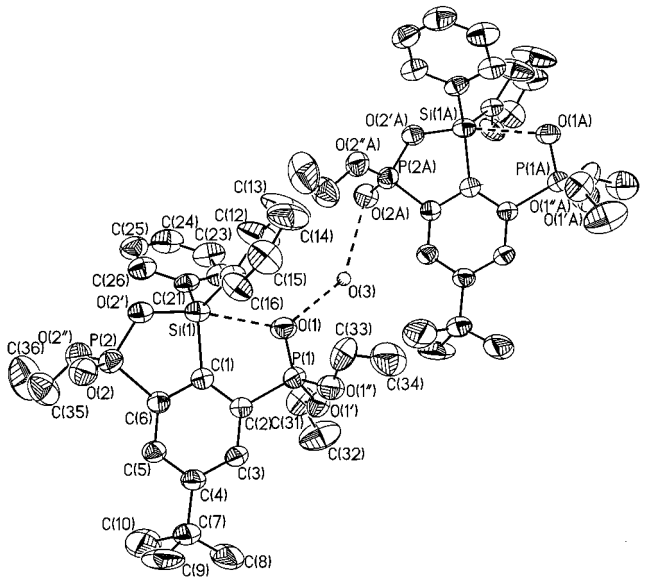

Figure 3. General view (SHELXTL) of a molecule of **5** showing 30% probability displacement ellipsoids and the atom numbering.

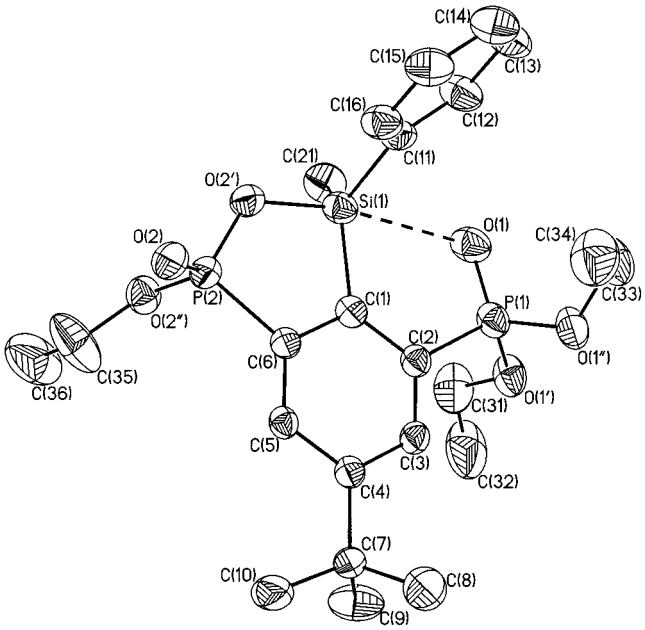

Figure 4. General view (SHELXTL) of a molecule of **6a** showing 30% probability displacement ellipsoids and the atom numbering. The other enantiomer is not shown.

Compound **5** crystallizes with 0.5 molar equiv of water (Figure 3). Each water molecule is linking two heterocycles via O(1)···H−O(3)−H···O(2a) bridges with O(1)−O(3) = 2.767(2) Å and O(2a)−O(3) = 2.887(2) Å.

The IR spectra show P=O absorptions at 1223 and 1256 cm^{-1} (**5**), 1217 and 1252 cm^{-1} (**6a**), and 1171 and 1251 cm^{-1} (**7**). The first two pairs correspond to P(1)−O(1) and P(2)−O(2) distances of 1.464(3) and 1.445(3) Å (**5**) and 1.467(2) and 1.457(2) Å (**6a**), respectively. For related benzoxaphosphastannole and benzoxaphosphaplumbole derivatives the corresponding P−O distances

(47) Van den Winkel, Y.; Bastiaans, H. M. M.; Bickelhaupt, F. *J. Organomet. Chem.* **1991**, *405*, 183.
(48) Van den Winkel, Y.; Bastiaans, H. M. M.; Bickelhaupt, F. *Phosphorus, Sulfur, Silicon Relat. Elem.* **1990**, *49/50*, 333.
(49) Peveling, K.; Schürmann, M.; Jurkschat, K. To be submitted for publication.

Table 4. Selected Bond Lengths (Å), Bond Angles (deg), and Torsion Angles (deg) for 5, 6a, and the Geometry-Optimized Structure of 6a (RHF 6-31G*)

	5	6a	6a (RHF 6-31G*)
Si(1)−C(1)	1.882(4)	1.884(3)	1.913
Si(1)−C(11)	1.844(4)	1.869(3)	1.877
Si(1)−C(21)	1.885(4)	1.850(3)	1.869
Si(1)−O(1)	2.672(3)	2.614(2)	2.877
Si(1)−O(2′)	1.715(3)	1.718(2)	1.702
P(1)−O(1)	1.464(3)	1.467(2)	1.464
P(2)−O(2)	1.445(3)	1.457(2)	1.457
P(1)−O(1′)	1.559(3)	1.569(2)	1.580
P(1)−O(1″)	1.556(3)	1.557(2)	1.571
P(2)−O(2′)	1.564(3)	1.563(2)	1.575
P(2)−O(2″)	1.592(3)	1.577(2)	1.585
C(11)−Si(1)−C(1)	119.0(2)	113.9(1)	116.1
C(21)−Si(1)−C(1)	118.6(2)	122.1(1)	117.5
C(21)−Si(1)−C(11)	115.0(2)	116.1(1)	115.6
C(1)−Si(1)−O(1)	76.1(2)	77.06(9)	74.2
O(2′)−Si(1)−C(1)	92.7(2)	92.7(1)	93.3
C(11)−Si(1)−O(1)	80.4(2)	84.8(1)	84.1
O(2′)−Si(1)−C(11)	102.3(2)	102.3(1)	104.4
C(21)−Si(1)−O(1)	86.2(2)	80.3(1)	78.7
O(2′)−Si(1)−C(21)	102.6(2)	103.2(1)	105.5
O(2′)−Si(1)−O(1)	168.2(1)	169.32(8)	167.2
O(1)−P(1)−C(2)	108.2(2)	108.1(1)	110.1
O(2′)−P(2)−C(6)	99.4(2)	99.3(1)	98.3
P(1)−O(1)−Si(1)	106.9(2)	107.0(1)	104.7
P(2)−O(2′)−Si(1)	120.4(2)	121.3(1)	121.7
P(2)−C(6)−C(1)	112.7(3)	113.2(2)	114.9
P(1)−C(2)−C(1)	116.2(3)	116.0(2)	119.3
C(6)−C(1)−Si(1)	113.2(3)	113.6(2)	111.7
C(2)−C(1)−Si(1)	130.0(3)	129.3(2)	131.4
C(5)−C(6)−C(1)−Si(1)	−176.6(3)	−177.9(2)	−178.3
C(3)−C(2)−C(1)−Si(1)	176.3(3)	177.3(2)	178.4
C(5)−C(6)−P(2)−O(2′)	−175.4(3)	177.7(2)	178.8
C(3)−C(2)−P(1)−O(1)	−164.1(3)	175.2(2)	175.2

Chart 2

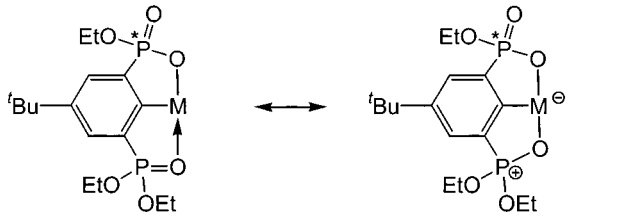

(I) (II)

5, M = $SiPh_2$, Δ(M-O) = 96 pm M = $SnPh_2$, Δ(M-O) = 27 pm

6, M = SiMePh, Δ(M-O) = 90 pm M = $PbPh_2$, Δ(M-O) = 17 pm

amount to 1.488(4) and 1.463(6) Å[29] and 1.524(7) and 1.451(7) Å,[49] respectively.

Selected NMR data for compounds **5**, **6a**, and **7** are given in Table 2.

The ^{29}Si NMR spectra of the benzoxasilaphospholes **5**−**7** show ABB'-type resonances at δ −24.7 ($J(^{29}Si-^{31}P)$ = 3, 7 Hz) (**5**), δ −5.3 ($J(^{29}Si-^{31}P)$ = 3, 6 Hz) and δ −6.4 ($J(^{29}Si-^{31}P)$ = 3, 6 Hz) (**6**, mixture of two diastereomers), and δ 10.5 ($J(^{29}Si-^{1}H)$ = 3, 6 Hz) (**7**). The ^{31}P NMR spectra show for each of the compounds **5**, **6a**, and **7** two equally intense resonances. The ^{31}P chemical shift differences $\Delta\delta$ of 0.4−1.9 between the two signals in each of the benzoxasilaphospholes are smaller than in the related organotin ($\Delta\delta$ = 11.3)[29] and organolead compounds ($\Delta\delta$ = 9.5).[49] Both the ^{1}H and the ^{13}C NMR spectra confirm for each compound the presence of three distinct ethoxy groups.

In $CDCl_3$ solution, compound **6a** undergoes slow epimerization. The process is acid-catalyzed; no epimerization takes place in both C_6D_6 and in C_6D_6 to which had been added a catalytic amount of $[(Ph_3P)_2N]^+Cl^-$. However, it does occur in C_6D_6 upon addition of a catalytic amount of *p*-$MeC_6H_4SO_3H$. The epimerization is slow on the ^{31}P NMR time scale and was studied by time-dependent ^{31}P NMR spectroscopy (Table 5 and Figure 5). After 8 days the mixture had been equilibrated. In agreement with the van't Hoff−Dimroth rule[50] the minor diastereomer **6a** crystallizes.

Table 5. Time-Dependent ^{31}P NMR Data for the Epimerization of 6a in Solution[a]

	c(6a)/c(6b)			
t, days	$CDCl_3$	C_6D_6	C_6D_6 + $[Ph_3P{=}N{=}PPh_3]^+Cl^-$	C_6D_6 + *p*-$MeC_6H_4SO_3H$
0	100/0	100/0		100/0
1	80/20	100/0	100/0	
2	71/29	100/0	100/0	
4	49/51			50/50
6			100/0	
8	43/57			

[a] Integration of the characteristic signals.

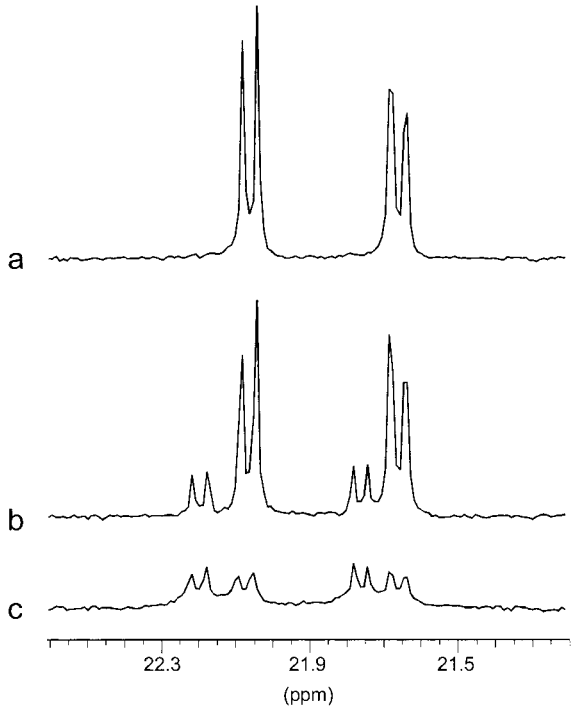

Figure 5. Time-dependent (a, t = 0; b, t = 1 day; c, t = 7.5 days) ^{31}P NMR spectra ($CDCl_3$, 64 scans for each measurement) of the epimerization process of **6a**.

One possible acid-catalyzed mechanism to account for the epimerization is shown in Scheme 2. The initial step involves protonation at either the exocyclic P=O or the endocyclic Si−O−P oxygen, followed by Si−O bond cleavage, rotation about the P−C bond, and re-formation of the Si−O bond under deprotonation, giving rise to inversion of configuration at phosphorus. Inversion of the configuration at the silicon atom is much less likely because of the strong intramolecular P=O→Si coordination in **6a′** (Scheme 2) preventing rotation about the Si−C(ligand) bond.

The proposed mechanism is supported by ab initio MO calculations. Selected geometrical data of the geometry-optimized structures of **6a**, of the P=O protonated

(50) Eliel, E. L.; Wilen, S. H.; Mander, L. N. *Stereochemistry of Organic Compounds*; Wiley-Interscience: New York, 1994.

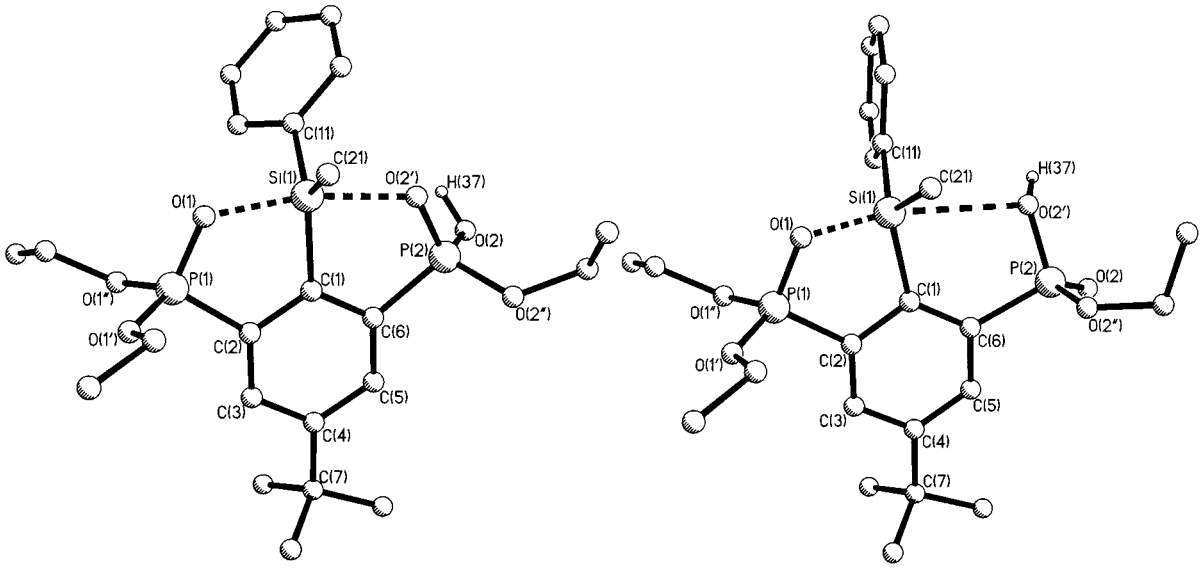

Figure 6. General view (SHELXTL) of the geometry-optimized hypothetical structures **6a1** and **6a2** resulting from protonation of **6a**.

Table 6. Selected Bond Lengths (Å), Bond Angles (deg), and Torsion Angles (deg) for the Geometry-Optimized Structure of 6a, the Structure Protonated at P═O(2) (6a1), and the Structure Protonated at Si−O(2′) (6a2)[a]

	6a	6a1	6a2
Si(1)−O(1)	2.877	1.915	1.782
Si(1)−O(2′)	1.702	2.035	2.831
P(2)−O(2″)	1.585	1.777	1.567
C(6)−C(1)−Si(1)	111.7	122.5	130.5
C(11)−Si(1)−O(1)	84.1	96.7	106.0
C(1)−C(2)−P(1)	119.3	110.6	112.8
C(5)−C(6)−P(2)−O(2′)	178.8	−174.9	163.3

[a] All optimizations were at the RHF 6-31G* level.

species **6a1**, and of the derivative protonated at the endocyclic Si−O−P oxygen, **6a2**, are given in Table 6. In comparison with the initial structure **6a**, protonation at either of the two oxygen atoms results in (i) a lengthening of the endocyclic Si(1)−O(2′) bond distance to 2.035 Å (**6a1**) and 2.831 Å (**6a2**) and (ii) a shortening of the intramolecular P═O→Si distance to 1.777 Å (**6a1**) and 1.567 Å (**6a2**) (Figure 6). Although the trend is the same for both **6a1** and **6a2**, it is more pronounced for the latter and suggests protonation at the endocyclic Si−O−P oxygen to be operative.

Conclusion

We have demonstrated the diversity of the pincer-type ligand $\{4\text{-}t\text{-Bu-2,6-}[P(O)(OEt)_2]_2C_6H_2\}^-$ in organosilicon chemistry. Interestingly, the [4 + 2] coordination mode of the ligand with both P═O donors pointing to the silicon atom in the tetraorganosilane **2** changes toward a [4 + 1] coordination mode upon replacement of one phenyl group by a hydrogen in the triorganosilane **3**. As for the related organotin derivatives, a variety of reactions are possible not only at the central metal atom but also at the phosphonyl moieties, giving rise to formation of intramolecularly coordinated benzoxasilaphospholes (**5**−**7**).

Experimental Section

General Considerations. All solvents were dried and purified by standard procedures. All reactions were carried out under a nitrogen atmosphere using Schlenk techniques.

IR spectra (cm^{-1}) were recorded on a Bruker IFS 28 spectrometer. Bruker DPX-300 and DRX-400 spectrometers were used to obtain ^1H, ^{13}C, ^{31}P, and ^{29}Si NMR spectra. ^1H, ^{13}C, ^{31}P, and ^{29}Si NMR chemical shifts δ are given in ppm and were referenced to Me_4Si and H_3PO_4 (85%). NMR spectra were recorded at room temperature unless otherwise stated. Elemental analyses were performed on a LECO-CHNS-932 analyzer. A satisfactory elemental analysis could not be obtained for compound **7**. However, its NMR spectra (Supporting Information) unambiguously support the identity of **7**.

[{2,6-Bis(diethoxyphosphonyl)-4-*tert*-butyl}phenyl]triphenylsilane (**2**) was prepared as previously reported.[32]

Ab Initio MO Calculations. Ab initio calculations were performed at the uncorrelated restricted Hartree−Fock (RHF) level for all structures using the Gaussian 94 program.[51] All calculations were carried out at the 3-21G and 6-31G* basis levels.[52] Due to computational limits larger basis sets were not taken into account. For comparability and consistency the largest structure ([{2,6-bis(diethoxyphosphonyl)-4-*tert*-butyl}-phenyl]triphenylsilane, containing 91 atoms) determined the limit for the chosen basis set. Further on we discuss the result for the largest 6-31G* basis set. This way we do not increase unnecessarily the amount of data and can concentrate on the features and characteristics of the molecular structures.

Crystallography. Intensity data for the colorless crystals were collected on a Nonius KappaCCD diffractometer with

(51) Frisch, M. J.; Trucks, G. W.; Schlegel, H. B.; Gill, P. M. W.; Johnson, B. G.; Robb, M. A.; Cheeseman, J. R.; Keith, T.; Petersson, G. A.; Montgomery, J. A.; Raghavachari, K.; Al-Laham, M. A.; Zakrzewski, V. G.; Ortiz, J. V.; Foresman, J. B.; Cioslowski, J.; Stefanov, B. B.; Nanayakkara, A.; Challacombe, M.; Peng, C. Y.; Ayala, P. Y.; Chen, W.; Wong, M. W.; Andres, J. L.; Replogle, E. S.; Gomperts, R.; Martin, R. L.; Fox, D. J.; Binkley, J. S.; Defrees, D. J.; Baker, J.; Stewart, J. P.; Head-Gordon, M.; Gonzalez, C.; Pople, J. A. *Gaussian 94*, revision A.1; Gaussian, Inc.: Pittsburgh, PA, 1995.

(52) For an authorative description of the ab initio methods and basis sets employed here, see: Hehre, W. G.; Radom, L.; Schleyer, P. v. R.; Pople, I. A. *Ab initio Molecular Orbital Theory*; Wiley: New York, 1986.

graphite-monochromated Mo Kα (0.71069 Å) radiation at 291 K. The data collection covered almost the whole sphere of reciprocal space with 360 frames via ω-rotation ($\Delta/\omega = 1°$) at 2 times 20 s (**3**), 80 s (**6a**), and 90 s (**5**) per frame. The crystal-to-detector distance was 2.8 cm (**6a**) and 3.00 cm (**3**, **5**) with a detector θ offset of 5° (**3**). Crystal decay was monitored by repeating the initial frames at the end of data collection. The data were not corrected for absorption effects. When the duplicate reflections were analyzed, there was no indication for any decay. The structure was solved by direct methods (SHELXS97[53]) and successive difference Fourier syntheses. Refinement applied full-matrix least-squares methods (SHELXL97[54]).

The H atoms of the phenyl rings of **6a** and the hydride at Si(1) of **3** were located in the difference Fourier map and refined isotropically. The other H atoms were placed in geometrically calculated positions using a riding model ($C-H_{prim} = 0.96$ Å, $C-H_{sec} = 0.97$ Å; $C-H_{aryl} = 0.93$). The isotropic temperature factors of the aliphatic H atoms of **5** are constrained to be 1.5 times those of the carrier atom. The H atoms of **3**, the aromatic H atoms of **5**, and the aliphatic H atoms of **6a** were refined with common isotropic temperature factors for H_{aryl} ($U_{iso} = 0.121(4)$ Å^2 (**3**), 0.114(5) Å^2 (**5**)) and for H_{alkyl} ($U_{iso} = 0.202(1)$ Å^2 (**3**), 0.191(4) Å^2 (**6a**)).

Disordered ethoxy (**5**) and *tert*-butyl (**3**, **5**) groups were found with occupancies of 0.4 (C(8′), C(9′), C(10′)) and of 0.6 (C(8), C(9), C(10)) in **3** and of 0.33 (C(9′)), 0.5 (C(33), C(33′)), and 0.66 (C(9)) in **5**. The water molecule (O(3)) in **5** was anisotropically refined with an occupancy of 0.5.

Atomic scattering factors for neutral atoms and real and imaginary dispersion terms were taken ref 55. The figures were created by SHELXTL.[56] Crystallographic data are given in Table 3 and selected bond distances and angles for **3** in Table 1 and for **5** and **6a** in Table 4.

[{2,6-Bis(diethoxyphosphonyl)-4-*tert*-butyl}phenyl]-hydridodiphenylsilane (3). Dichlorodiphenylsilane (1.40 g, 6.40 mmol) was added dropwise, at −65 °C, to a solution of [2,6-bis(diethoxyphosphonyl)-4-*tert*-butyl]phenyllithium (**1**; 2.53 g, 6.14 mmol) in diethyl ether (50 mL). The reaction mixture was stirred for 16 h (−65 °C to room temperature), and then the solvent was evaporated. Column chromatography (SiO_2/EtOAc) of the residue afforded 2.48 g (69%) of **3** as a colorless solid, mp 78−80 °C. ^{1}H NMR (400.13 MHz, $CDCl_3$): δ 0.96 (t, 12H; CH_3), 1.23 (s, 9H; CH_3), 3.73−3.83 (complex pattern, 4H; CH_2), 3.88−3.97 (complex pattern, 4H; CH_2), 6.59 (s, $^1J(^1H-^{29}Si)$ = 196 Hz, 1H; Si−H), 7.28 (complex pattern, 6H; aromatics), 8.15 (complex pattern, 4H; aromatics), 8.68 (complex pattern, 2H; aromatics). $^{13}C\{^1H\}$ NMR (100.63 MHz, $CDCl_3$): δ 15.9 (t, 4C; CH_3), 30.9 (s, 3C; CH_3), 34.9 (s, 1C; C), 61.8 (dd, $^2J(^{13}C-^{31}P) = 3$ Hz, $^2J(^{13}C-^{31}P) = 2$ Hz, 4C; CH_2), 127.1 (s, 4C; C_m), 128.5 (s, 2C; C_p), 134.1 (complex pattern, 2C; $C_{3,5}$), 135.3 (s, 4C; C_o), 136.0 (s, 2C; C_i), 138.1 (dd, $^1J(^{13}C-^{31}P) = 189$ Hz, $^3J(^{13}C-^{31}P) = 19$ Hz, 2C; $C_{2,6}$), 140.7 (1C; C_1), 151.8 (t, 1C; C_4). ^{29}Si NMR (59.63 MHz, CH_2Cl_2/ D_2O-capillary): δ −25.6 (dt, $J(^{29}Si-^{31}P) = 5$ Hz, $^1J(^{29}Si-^1H = 196$ Hz). $^{31}P\{^1H\}$ NMR (161.98 MHz, $CDCl_3$): δ 19.8. IR (Nujol): $\tilde{\nu}$(P=O) 1251 cm^{-1}, $\tilde{\nu}$(Si−H) 2198 cm^{-1}. Anal. Calcd for $C_{30}H_{42}O_6SiP_2$: C, 61.2; H, 7.2. Found: C, 61.3; H, 7.4. MS: *m*/*z* (%) 588 (40, M), 587 (100, M − H), 510 (44, M − Ph − H), 437 (60, M − Ph − O − H − *t*-Bu).

In Situ Generation of [{2,6-Bis(diethoxyphosphonyl)-4-*tert*-butyl}phenyl]diphenylsiliconium Ion (Cation of 4). Method A. To a solution of [{2,6-bis(diethoxyphosphonyl)-4-*tert*-butyl}phenyl]triphenylsilane (**2**; 0.21 g, 0.32 mmol) in toluene (5 mL) was added, at 55 °C, triphenylcarbonium hexafluorophosphate (0.16 g, 0.41 mmol). The reaction mixture was stirred at this temperature for 4 days and then the solvent was evaporated to give a brown oil. The latter was extracted four times with 10 mL of hexane. The colorless residue was characterized by NMR spectroscopy. ^{1}H NMR (400.13 MHz, C_6D_6): δ 1.01 (t, 12H; CH_3), 1.47 (s, 9H; CH_3), 3.96−4.01 (complex pattern, 4H; CH_2), 4.07−4.11 (complex pattern, 4H; CH_2), 7.23−7.27 (complex pattern, 2H; aromatics) 7.27−7.34 (complex pattern, 4H; aromatics), 7.98 (complex pattern, 4H; aromatics), 8.58 (m, 2H; aromatics). $^{29}Si\{^1H\}$ NMR (79.49 MHz, C_6D_6): δ −67.9 (t, $J(^{29}Si-^{31}P) = 2$ Hz). $^{31}P\{^1H\}$ NMR (162.00 MHz, C_6D_6): δ 29.6.

Method B. To a solution of [{2,6-bis(diethoxyphosphonyl)-4-*tert*-butyl}phenyl]hydridodiphenylsilane (**3**; 0.60 g, 1.02 mmol) in toluene (20 mL) was added, at 0 °C, triphenylcarbonium hexafluorophosphate (0.38 g, 0.98 mmol). The reaction mixture was stirred for 3 days at 68 °C, followed by evaporation of the solvent in vacuo. The resulting brown residue was characterized by NMR spectroscopy.

6-*tert*-Butyl-4-(diethoxyphosphonyl)-1-ethoxy-1-oxo-3,3-diphenyl-2,3,1-benzoxasilaphosphole (5). Method A. To a solution of [{2,6-bis(diethoxyphosphonyl)-4-*tert*-butyl}-phenyl]hydridodiphenylsilane (**3**; 0.60 g, 1.02 mmol) in toluene (20 mL) was added, at 0 °C, triphenylcarbonium hexafluorophosphate (0.38 g, 0.98 mmol). After the reaction mixture was stirred for 3 days at 68 °C, the solvent was evaporated and the residual brown oil was exposed to atmospheric moisture for 7 days. Column chromatography (SiO_2/EtOAc) of the residue and crystallization from hexane afforded 0.21 g (38%) of **5** as a colorless solid, mp 160 °C. ^{1}H NMR (400.13 MHz, $CDCl_3$): δ 0.92 (t, 3H; CH_3), 1.10 (t, 3H; CH_3), 1.22 (t, 3H; CH_3), 1.37 (s, 9H; CH_3), 3.40−3.60 (complex pattern, 2H; CH_2), 3.63−3.85 (complex pattern, 2H; CH_2), 4.06−4.13 (complex pattern, 2H; CH_2), 7.28−7.39 (complex pattern, 6H; aromatics), 7.85 (d, 1H; aromatics), 7.87 (complex pattern, 4H; aromatics), 8.16 (d, 1H; aromatics). $^{13}C\{^1H\}$ NMR (100.63 MHz, $CDCl_3$): δ 15.9 (d, $^3J(^{13}C-^{31}P) = 6$ Hz; CH_3), 16.1 (d, $^3J(^{13}C-^{31}P) = 6$ Hz; CH_3), 16.4 (d, $^3J(^{13}C-^{31}P) = 6$ Hz; CH_3), 31.0 (s, 3C; CH_3), 35.3 (s, 1C; C), 62.5 (d, $^2J(^{13}C-^{31}P) = 6$ Hz; CH_2), 62.7 (complex pattern; CH_2), 127.5 (s, 2C; C_m), 127.4 (s, 2C; C_m), 129.8/131.1 (dd/dd, $^2J(^{13}C-^{31}P) = 13$ Hz/$^2J(^{13}C-^{31}P) = 12$ Hz, $^4J(^{13}C-^{31}P) = 3$ Hz/$^4J(^{13}C-^{31}P) = 3$ Hz, 2C; $C_{5,7}$), 130.0 (s, 1C; C_p), 130.1 (s, 1C; C_p), 132.6 (complex pattern, 1C; C_i), 132.6/139.5 (dd/dd, $^1J(^{13}C-^{31}P) = 184$ Hz/$^1J(^{13}C-^{31}P) = 178$ Hz, $^3J(^{13}C-^{31}P) = 18$ Hz/$^3J(^{13}C-^{31}P) = 16$ Hz, 2C; $C_{4,9}$), 133.5 (complex pattern, 1C; C_i), 135.2 (s, 1C; C_o), 136.1 (s, 1C; C_o), 144.8 (dd, $^2J(^{13}C-^{31}P) = 19$ Hz/$^2J(^{13}C-^{31}P) = 25$ Hz, 1C; C_8), 155.5 (t, $^3J(^{13}C-^{31}P) = 13$ Hz, 1C; C_6). $^{29}Si\{^1H\}$ NMR (79.49 MHz, $CDCl_3$): δ −24.7 (dd, $J(^{29}Si-^{31}P) = 3/7$ Hz). $^{31}P\{^1H\}$ NMR (161.98 MHz, $CDCl_3$): δ 21.48 (d, $^4J(^{31}P-^{31}P) = 6$ Hz , $^1J(^{13}C-^{31}P) = 176$ Hz), 22.45 (d, $^4J(^{31}P-^{31}P) = 6$ Hz, $^1J(^{13}C-^{31}P) = 183$ Hz). IR (KBr): $\tilde{\nu}$(P=O) 1223, 1256 cm^{-1}; $\tilde{\nu}$(OH) 3479, 3525 cm^{-1}. Anal. Calcd for $C_{28}H_{36}O_6SiP_2 \cdot 0.5H_2O$: C, 59.3; H, 6.6. Found: C, 59.6; H, 6.2. MS: *m*/*z* (%) 558 (28, M), 482 (29, M − Ph + H), 481 (100, M − Ph), 453 (11, M − ^{t}Bu − OEt − 3H).

Method B. To a solution of [{2,6-bis(diethoxyphosphonyl)-4-*tert*-butyl}phenyl]triphenylsilane (**2**; 0.21 g, 0.32 mmol) in toluene (5 mL) was added, at 55 °C, triphenylcarbonium hexafluorophosphate (0.16 g, 0.41 mmol). After the reaction mixture was stirred for 4 days at this temperature, the solvent was evaporated. The residual brown oil was extracted four times with 10 mL of hexane, in order to remove unreacted **2**, and exposed to atmospheric moisture for 3 days. The crude reaction product was dissolved in C_6D_6 and studied by ^{31}P NMR spectroscopy, revealing formation of compound **5** in 80% yield.

Method C. To a solution of [2,6-bis(diethoxyphosphonyl)-4-*tert*-butyl]phenyllithium (**1**; 2.25 g, 5.46 mmol) in diethyl ether (50 mL) was added portionwise, at −70 °C, dichlorodiphenylsilane (1.67 g, 6.46 mmol). The reaction mixture was

(53) Sheldrick, G. M. *Acta Crystallogr.* **1990**, *A46*, 467.
(54) Sheldrick, G. M. SHELXL97; University of Göttingen, Göttingen, Germany, 1997.
(55) *International Tables for Crystallography*; Kluwer Academic: Dordrecht, The Netherlands, 1992; Vol. C.
(56) Sheldrick, G. M. *SHELXTL. Release 5.1 Software Reference Manual*; Bruker AXS: Madison, WI, 1997.

stirred for 16 h (−65 °C to room temperature) and then heated at reflux for further 9 h. The reaction mixture was filtered in order to remove the lithium chloride. The filtrate was evaporated in vacuo and the residue dissolved in C_6D_6. The ^{31}P NMR spectrum of this solution revealed formation of compound **5** in 18% yield.

(1*S,3*S**)-6-*tert*-Butyl-4-(diethoxyphosphonyl)-1-ethoxy-1-oxo-3-methyl-3-phenyl-2,3,1-benzoxasilaphosphole (6a).** Dichloromethylphenylsilane (1.14 mL, 6.98 mmol) was added portionwise, at −65 °C, to a solution of [2,6-bis(diethoxyphosphonyl)-4-*tert*-butyl]phenyllithium (**1**; 2.39 g, 5.80 mmol) in diethyl ether (50 mL). The reaction mixture was stirred for 4 days (−65 °C to room temperature), followed by heating at reflux for 5 h. The solvent was evaporated. Column chromatography (SiO_2/EtOAc) of the residue and extraction with hexane afforded 1.13 g (39%) of **6** as a colorless oil. Recrystallization from hexane afforded 0.21 g (7%) of **6a** as a colorless solid, mp 107−109 °C. ^1H NMR (400.13 MHz, $CDCl_3$): δ 0.80 (t, 3H; CH_3), 0.92 (s, 3H; $SiCH_3$), 1.30 (t, 3H; CH_3), 1.36 (t, 3H; CH_3), 1.36 (s, 9H; CH_3), 3.16−3.36 (complex pattern, 2H; CH_2), 3.95−4.24 (complex pattern, 4H; CH_2), 7.26−7.35 (complex pattern, 3H; aromatics), 7.75 (dd, $J(^1H-^{31}P) = 8$ Hz, 2H; aromatics), 7.82 (dt, $J(^1H-^{31}P) = 14$ Hz, 1H; aromatics), 8.11 (dt, $J(H-^{31}P) = 13$ Hz, 1H; aromatics). $^{13}C\{^1H\}$ NMR (100.63 MHz, $CDCl_3$): δ −1.8 (t, $J(^{13}C-^{31}P) = 2$ Hz, 1C; $SiCH_3$), 15.8 (d, $^3J(^{13}C-^{31}P) = 6$ Hz; CH_3), 16.2 (d, $^3J(^{13}C-^{31}P) = 6$ Hz; CH_3), 16.5 (d, $^3J(^{13}C-^{31}P) = 6$ Hz, CH_3), 31.0 (s, 3C; CH_3), 35.2 (s, 1C; C), 62.1 (d, $^2J(^{13}C-^{31}P) = 4$ Hz; CH_2), 62.4 (complex pattern; CH_2), 127.4 (s, 2C; C_m), 129.3/131.5 (dd/dd, $^2J(^{13}C-^{31}P) = 14$ Hz/$^2J(^{13}C-^{31}P) = 12$ Hz, $^4J(^{13}C-^{31}P) = 4$ Hz/$^4J(^{13}C-^{31}P) = 3$ Hz, 2C; $C_{5,7}$), 130.0 (s, 1C; C_p), 132.5/138.6 (dd/dd, $^1J(^{13}C-^{31}P) = 186$ Hz/$^1J(^{13}C-^{31}P) = 179$ Hz, $^3J(^{13}C-^{31}P) = 17$ Hz/$^3J(^{13}C-^{31}P) = 16$ Hz, 2C, $C_{4,9}$), 133.8 (d, $J(^{13}C-^{31}P) = 4$ Hz, 1C; C_i), 134.8 (s, 2C; C_o), 145.11 (dd, $^2J(^{13}C-^{31}P) = 19$ Hz/$^2J(^{13}C-^{31}P) = 26$ Hz, 1C; C_8), 155.0 (t, $^3J(^{13}C-^{31}P) = 12$ Hz, 1C; C_6). $^{29}Si\{^1H\}$ NMR (79.49 MHz, $CDCl_3$): δ −5.3 (dd, $J(^{29}Si-^{31}P) = 3/6$ Hz). $^{31}P\{^1H\}$ NMR (162.00 MHz, $CDCl_3$): δ 21.66 (d, $^4J(^{31}P-^{31}P) = 6$ Hz), 22.06 (d, $^4J(^{31}P-^{31}P) = 6$ Hz). IR (KBr): $\tilde{\nu}$(P═O) 1217 cm^{-1}, 1252 cm^{-1}. Anal. Calcd for $C_{23}H_{34}O_6SiP_2$: C, 55.6; H, 6.9. Found: C, 55.5; H, 7.0. MS: *m*/*z* (%) 496 (18, M), 481 (30, M − O + H), 480 (100, M − O), 453 (10, M − OEt + 2H), 439 (1, M − ^{t}Bu), 419 (32, M − Ph), 397 (10, M − ^{t}Bu − OEt + 3H).

***tert*-Butyl-4-(diethoxyphosphonyl)-1-ethoxy-1-oxo-3,3-dimethyl-2,3,1-benzoxasilaphosphole (7).** Dichlorodimethylsilane (1.10 mL, 9.14 mmol) was added portionwise, at −65 °C, to a solution of [2,6-bis(diethoxyphosphonyl)-4-*tert*-butyl]-phenyllithium (**1**; 3.03 g, 7.34 mmol) in diethyl ether (50 mL). The reaction mixture was stirred overnight, reaching room temperature, and was then heated at reflux for 7 h. After separation by filtration of the lithium chloride formed, the residue was washed with CH_2Cl_2. The combined filtrates were evaporated in vacuo to give an oily residue which was washed several times with *n*-hexane in order to remove unreacted Me_2SiCl_2 and [1,3-bis(diethoxyphosphonyl)-5-*tert*-butyl]benzene, the latter being formed by hydrolysis of unreacted **1**. Finally, the oil was stripped off in vacuo (10^{-3} mm/Hg) from residual amounts of solvent to give 1.44 g (45%) of **7** as a colorless oil. ^1H NMR (400.13 MHz, C_6D_6): δ 0.84 (s, 3H; CH_3), 0.89 (s, 3H; CH_3), 0.95 (m, 6H; CH_3), 1.08 (s, 9H; CH_3), 1.17 (t, 3H; CH_3), 3.60−3.75 (complex pattern, 2H; CH_2), 3.75−3.91 (complex pattern, 2H; CH_2), 4.17−4.30 (complex pattern, 2H; CH_2), 7.96 (d, 1H; aromatics), 8.32 (d, 1H; aromatics).$^{13}C\{^1H\}$ NMR (100.63 MHz, C_6D_6): δ 0.59 (s, 1C; $SiCH_3$), 0.90 (s, 1C; $SiCH_3$), 16.21 ppm (d, $^3J(^{13}C-^{31}P) = 6$ Hz; CH_3), 16.75 (d, $^3J(^{13}C-^{31}P) = 6$ Hz; CH_3), 30.78 (s, 3C; CH_3), 34.95 (s, 1C; C), 62.26 (complex pattern; CH_2), 129.90/131.03 (dd/dd, $^2J(^{13}C-^{31}P) = 14$ Hz/$^2J(^{13}C-^{31}P) = 12$ Hz, $^4J(^{13}C-^{31}P) = 3$ Hz/$^4J(^{13}C-^{31}P) = 3$ Hz, 2C; $C_{5,7}$), 132.95/140.67 (dd/dd, $^1J(^{13}C-^{31}P) = 185$ Hz/$^1J(^{13}C-^{31}P) = 178$ Hz, $^3J(^{13}C-^{31}P) = 18$ Hz/$^3J(^{13}C-^{31}P) = 17$ Hz, 2C; $C_{4,9}$), 146.92 (dd, $^2J(^{13}C-^{31}P) = 20$ Hz/$^2J(^{13}C-^{31}P) = 27$ Hz, 1C; C_8), 154.82 (t, $^3J(^{13}C-^{31}P) = 12$ Hz, 1C; C_6). $^{29}Si\{^1H\}$ NMR (79.49 MHz, $CDCl_3$): δ 10.5 (dd, $J(^{21}Si-^{31}P) = 3/6$ Hz). $^{31}P\{^1H\}$ NMR (161.98 MHz, C_6D_6): δ 19.9 (d, $^4J(^{31}P-^{31}P) = 6$ Hz), 21.8 (d, $^4J(^{31}P-^{31}P) = 6$ Hz). IR (Nujol): $\tilde{\nu}$(P═O) 1171, 1251 cm^{-1}. Anal. Calcd for $C_{18}H_{32}O_6SiP_2$: C, 49.8; H, 7.4. Found: C, 48.7; H, 7.4. MS: *m*/*z* (%) 434 (9, M), 420 (26, M − Me + H), 419 (100, M − Me), 389 (3, M − OEt), 317 (8, M − ^{t}Bu − O − OEt + H), 301 (4, M − ^{t}Bu − O − OEt − Me), 239 (2, M − ^{t}Bu −P(O)(OEt)$_2$ − H).

Acknowledgment. We thank the Deutsche Forschungsgemeinschaft and the Fonds der Chemischen Industrie for financial support.

Supporting Information Available: Tables of all atomic coordinates, anisotropic displacement parameters, and geometric data for compounds **3**, **5**, and **6a**, tables of Hartree−Fock Cartesian coordinates for compounds **2**, **3**, **3′**, **6a**, **6a1**, and **6a2** and figures giving ^1H, ^{13}C, ^{29}Si, and ^{31}P NMR spectra of compound **7**. This material is available free of charge via the Internet at http://pubs.acs.org.

OM010334C